JCTC Journal of Chemical Theory and Computation

Article

pubs.acs.org/JCTC

Assessing the Accuracy of Various Ab Initio Methods for Geometries and Excitation Energies of Retinal Chromophore Minimal Model by Comparison with CASPT3 Results

Dawid Grabarek, Elżbieta Walczak, and Tadeusz Andruniów*

Advanced Materials Engineering and Modelling Group, Wroclaw University of Technology, Wyb. Wyspianskiego 27, 50-370 Wroclaw, Poland

Supporting Information

ABSTRACT: The effect of the quality of the ground-state geometry on excitation energies in the retinal chromophore minimal model (PSB3) was systematically investigated using various single- (within Møller−Plesset and coupled-cluster frameworks) and multiconfigurational [within complete active space self-consistent field (CASSCF) and CASSCF-based perturbative approaches: second-order CASPT2 and third-order CASPT3] methods. Among investigated methods, only CASPT3 provides geometry in nearly perfect agreement with the CCSD(T)-based equilibrium structure. The second goal of the present study was to assess the performance of the CASPT2 methodology, which is popular in computational spectroscopy of retinals, in describing the excitation energies of low-lying excited states of PSB3 relative to CASPT3 results. The resulting CASPT2 excitation energy error is up to 0.16 eV for the $S_0 \rightarrow S_1$ transition but only up to 0.06 eV for the $S_0 \rightarrow S_2$ transition. Furthermore, CASPT3 excitation energies practically do not depend on modification of the zeroth-order Hamiltonian (so-called IPEA shift parameter), which does dramatically and nonsystematically affect CASPT2 excitation energies.

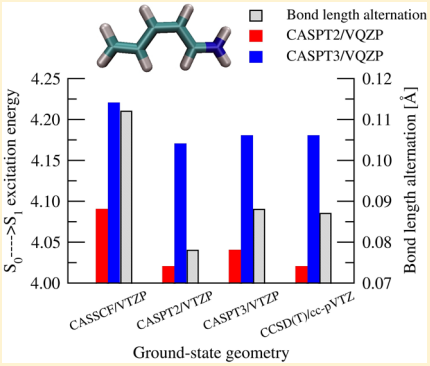

1. INTRODUCTION

Retinylidene proteins (also commonly called rhodopsins) use the retinal molecule as their chromophore, which is covalently linked through a protonated iminium moiety to the highly conserved lysine residue. Thus, this form of retinal is usually called retinal protonated Schiff base (RPSB). They are found in many organisms, ranging from archaea through algae and invertebrates up to humans.[1−3] They act as visual pigments (rhodopsin, photopsins) and they control pupillary light reflex and circadian photoentrainment (melanopsin) in higher organisms. In microorganisms, they are responsible for detection of light and phototaxis (sensory rhodopsins) as well as for light-driven, active transport of chloride ions (halorhodopsin) or protons (bacteriorhodopsin).

The biological activity of rhodopsins comes from stereoselective photoisomerization of retinal. This is one of the fastest (the first photointermediate in the visual rhodopsin cycle is formed in merely 200−250 fs)[4−6] and most efficient (quantum yield of ca. 0.65)[7,8] processes known to date. Due to these features, both microbial and animal rhodopsins find applications in modern technologies, e.g., in construction of artificial retinas or photovoltaic devices, memory storage, and readout.[3,9,10] They also serve as model systems with the ultimate goal of designing photoswitching organic molecules.[11,12]

Although the retinal photoisomarization event has been a subject of extensive experimental studies,[5,13−21] gaining insight into the photoisomerization mechanism as well as the role of the protein environment requires a theoretical chemistry approach due to the remarkable rate of this process and complex interactions between the RPSB and protein cavity residues.

It was found that retinal chromophore can be successfully described with single-reference methods, such as the second-order Møller−Plesset perturbation theory (MP2)[22] in the ground electronic state (S_0).[23−25] However, for reliable calculations of geometric, electronic, and spectral properties in both ground (e.g., far from the equilibrium geometry) and excited states, multireference methods are required. What is more, according to recent reports, a balanced description of both static and dynamic correlations should be provided for the most reliable results.[24] For the last two decades, a widely used computational method to investigate the photoisomerization mechanism of various retinal models and derivatives either in the gas phase[26−34] or in the protein environment[35−39] has been the CASPT2//CASSCF scheme, which is a two-step procedure starting from geometry optimization within a CASSCF[40] framework followed by calculating the CASPT2[41] correction to the energy that accounts for the dynamic correlation energy missing in CASSCF calculations. Such an approach often utilizes 6-31G* basis set. However, it has been recently reported that the CASPT2//CASSCF/6-31G* approach draws from fortuitous cancellation of errors, as the CASSCF geometry is less reliable than the CASPT2 one.[23,24,42] Page and

Received: January 29, 2016
Published: April 6, 2016

DOI: 10.1021/acs.jctc.6b00108
J. Chem. Theory Comput. 2016, 12, 2346−2356

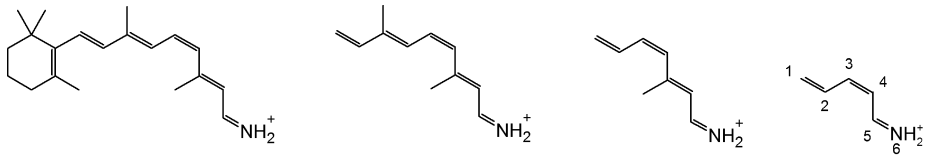

Figure 1. Exemplary RPSB models differing in a length of the conjugated double bonds' system. The 11-*cis* RPSB is a full model. Heavy atom numbering of the investigated PSB3 model is also shown.

Olivucci[43] were the first to show that the CASSCF/6-31G* and CASPT2/6-31G* ground- and excited-state (GS and ES, respectively) geometries of small organic molecules (including RPSB models) significantly differ. In another study by Valsson et al.,[24] it has also been demonstrated that the CASSCF methodology gives significantly longer single bonds and shorter double bonds in the ground state of PSB3, compared to the CASPT2 and quantum Monte Carlo (QMC) approaches. What is more, the authors report that after excitation to the first excited state (S_1) and in-plane relaxation (with constrained torsional angles), the excited-state structures obtained with CASPT2, full and approximate coupled cluster singles and doubles methods (CCSD and CC2, respectively)[44,45] and QMC approaches agree quite well, while they are significantly in variance with those obtained with the CASSCF method. This seems to be true not only for the minimal model but also for PSB4 and PSB5 models, i.e., retinal models with four or five double bonds, respectively (Figure 1). Similar conclusions were drawn by Olivucci's group,[46] based on minimum energy pathways of PSB3 photoisomerization, that inclusion of dynamic correlation effects either variationally or perturbatively has a significant qualitative impact on the shape of the S_1 potential energy surface (PES) near the conical intersection (CI) with the S_0 PES. It seems that dynamic correlation significantly stabilizes the charge-transfer character of the minimal model compared to the covalent-diradical structure. Although, this has a significant impact on the statistics and quantitative properties of the photoisomerization, its general mechanism is properly described by the CASSCF approach.[46]

The CASPT2 approach seems to be the desired one to obtain the geometries of retinal models in both the ground state and the excited states. However, it is computationally expensive, and so far only numerical CASPT2 gradients are available.[47] Moreover, CASPT2 excitation energies suffer from large errors, up to 0.35 eV, when the corrected zero-order Hamiltonian (IPEA shift)[48] is not employed.[23−25] Oddly enough, the CASPT2//CASSCF/6-31G* protocol does perform well only without the IPEA correction. The plausible explanation for its good performance is the cancellation of errors coming from overestimation of the excitation energies by utilization of a relatively small basis set and underestimation by not including the IPEA correction.[23,24,46]

Interestingly, results of the photoisomarization studies found with the CASPT2 approach seem to be consistent with the CC2 results published by Send and co-workers[49−52] and supported by Valsson et al.[24] Although the CC2 method can be utilized to treat systems in the excited state, it is still a single-reference method, and therefore, it has been considered as not being able to properly describe the vicinity of a true conical intersection between the ground electronic state and the first response state. Surprisingly, in a recent paper, Tuna et al.[53] revealed that it is possible, at least for PSB3 retinal model. However, in the surface crossing region, CC2 calculations are prone to artifacts, and more studies are needed to establish CC2 suitability for full reaction path or dynamics calculations in the excited states.

Currently, within multireference and coupled cluster ansatz, only the lowest levels of theory methods (CASSCF and CC2, respectively) are available to describe both ground and excited states of full retinals, especially inside the protein environment. Therefore, it is of utmost importance to establish the accuracy of these approaches with respect to the results produced by high-level theory methods, e.g. CASPT2, CASPT3, and coupled cluster with single and double excitations and perturbative correction for triple excitations (CCSD(T)). A perfect candidate for such studies is the minimal retinal model—PSB3. Although the PSB3 model is significantly truncated and lacks the structural features of the full model (methyl substituents, six-membered β-ionone ring, longer system of the conjugated double bonds; see Figure 1) that are important for quantitative spectral properties of the retinal, the minimal model is still extensively used to gain qualitative insight into RPSB properties and the photoisomerization mechanism.[26,34,46,52,54−57]

The objective of the present work is two-fold: (i) to assess the performance of various single- and multireference ab initio methods extensively used in computations of the ground-state geometry of retinals, e.g., MP2, CC2, CASSCF, and CASPT2 methods with respect to the CASPT3 as well as to the reference CCSD(T) data with a special emphasis on the impact of the choice of the ground-state geometry on excitation energies and (ii) to investigate the reliability of the CASPT2- and CASPT2//CASSCF-based excitation energies in terms of CASPT3 results. To the best of our knowledge, this is the first attempt to investigate the spectroscopy of the retinal model using the high-level CASPT3 method. Moreover, PSB3 is presumably the largest molecular system of which the ground-state geometry has been optimized using the CASPT3 methodology (for CASPT3 calculations on other molecular systems, see refs 58−63). Specifically, the ground-state geometry of the minimal model of retinal (PSB3) is extensively studied by various methods within the complete active space (CASSCF), multireference perturbation theory (CASPT2, CASPT3), Møller−Plesset perturbation theory (MP2, MP3, MP4), and coupled cluster ansatz (CC2, CCSD, CCSD(T)). Basis sets ranging from double- to quadruple-ζ quality are used for the geometry optimization and subsequent CASPT2 and CASPT3 calculations of excitation energies. The impact of the modifications to the effective Hamiltonian by the usage of the IPEA shift parameter on the CASPT2- and CASPT3-based excitation energies is also discussed.

2. METHODOLOGY

2.1. Ground-State Geometry Optimization. The CASSCF and CASPT2 GS geometries of the PSB3 model (Figure 1) were optimized with Molcas 7.6,[64] while CASPT3

DOI: 10.1021/acs.jctc.6b00108
J. Chem. Theory Comput. 2016, 12, 2346−2356

ones with Molpro 2012.1[65] computational packages. The 6-31G*[66] and ANO-L-VXZP (atomic natural orbitals-large-valence X-tuple-ζ polarizable, where X = D, T, Q; VQZP used only in CASSCF and CASPT2) basis sets were used. The ANO basis sets are generally contracted basis sets, specially optimized for the Molcas suite of programmes.[67−69] In CASSCF and both multireference perturbation theory calculations (CASPT2, CASPT3), the active space consisted of six active π orbitals and six electrons. The CASSCF and CASPT2 ground-state geometries were optimized using the frozen-core approximation, i.e., heavy atoms' 1s orbitals were frozen. Relaxed core or frozen core schemes selection in the CASSCF and CASPT2 optimization procedures does affect the resulting equilibrium geometry only marginally (bond lengths differences are less than 3×10^{-4} Å). Also, the Cholesky decomposition algorithm for two-electron integrals evaluation was used with the default threshold of 10^{-4}. In the case of the CASPT2 geometry optimization, the S-IPEA correction (0.25 hartree) was utilized. It was also confirmed that the CASPT2 structures optimized with no IPEA correction (0-IPEA) do not differ in bond lengths by more than 0.001 Å. In the case of the CASPT3 optimization, neither the frozen core approximation nor S-IPEA parameter was used. To the best of our knowledge, the CASPT3 GS geometries of the retinal PSB3 model are reported for the very first time.

The Møller−Plesset (MP2, MP3, MP4), CCSD, and CCSD(T) GS geometries were obtained with the Gaussian09 revision D01 computational package.[70] In fact, the MP4(SDQ) approach, instead of a true MP4 method, was used, i.e., single, double, and quadruple excitations were only included. The 6-31G* basis set and correlation-consistent polarizable valence X-tuple-ζ (cc-pVXZ, where X = D, T, Q; cc-pVQZ used only in CC2 and MP2) basis sets were used.[71]

The CC2 geometries were optimized with the Turbomole 6.5 computational package.[72] Resolution of the identity (RI) approximation was employed for more efficient calculations.[73] For optimization in the 6-31G* basis set, the cc-pVDZ auxiliary basis set GS geometry was used. At single-determinant levels of theory, no core orbitals were frozen.

2.2. Energetic Properties. The excitation energies were calculated with the CASPT2 method in ANO-L-VDZP, ANO-L-VTZP, and ANO-L-VQZP basis sets utilizing the Molcas 7.6 computational package.[64] Calculations were performed for both 0-IPEA and S-IPEA parameters, for CASSCF(6,6) reference wave functions averaged over either two or three states (roots), and employing either single-state (SS-CASPT2) or multistate (MS-CASPT2) protocols.[74] All MS-CASPT2 results as well as multireference perturbation calculations using the two-roots SA-CASSCF wave function (SS-CASPT2, MS-CASPT2, and CASPT3) are shown in Tables S1−S7 of the Supporting Information. To rule out intruder states, an imaginary shift[75] of 0.1 hartree was used for calculations in triple- and quadruple-ζ basis sets. Unless indicated, CASPT2 excitation energies were obtained using the SS-CASPT2 protocol with the S-IPEA parameter.

CASPT3 excitation energies were calculated in ANO-L-VDZP, ANO-L-VTZP, and ANO-L-VQZP basis sets with the Molpro 2010.1 program.[65] Calculations were performed using the CASSCF(6,6) wave function averaged over three states. Single-state CASPT3 protocol was utilized. The S-IPEA parameter and imaginary shift equal to 0.1 hartree were used. For chosen geometries, 0-IPEA was also checked to investigate the IPEA influence on the excitation energies (Tables S8 and S9, Supporting Information). Calculations of excitation energies were carried out with the frozen core approximation.

MR-CISD and cc-pVDZ properties were calculated with the Molpro 2010.1[65] program. The reference wave function for MR-CISD energies was the CASSCF(6,6) wave function averaged over three states. Besides "plain" MR-CISD energies, also Davidson[76] and Pople[77] corrections, to account for quadruple excitations and improve size consistency of MR-CISD methodology, were calculated (Tables S10 and S11, Supporting Information). In the main text only, MR-CISD excitation energies with the Pople correction are presented.

One-electron properties like oscillator strengths or changes in dipole moments of the excited states relative to the dipole moment of the ground state based on the SA-CASSCF wave function were also calculated and are shown in Figures S4−S7 and S10 and Tables S12−S20 of the Supporting Information.

3. MOLECULAR STRUCTURES

3.1. Basis Set Size Impact. Impact of the basis set size on the PSB3 bond lengths within a given ansatz is discussed here (Figure S1, Supporting Information).

Increasing the basis set size from 6-31G* to cc-pVDZ makes all bonds longer within 0.006−0.009 Å in the coupled cluster levels of theory. The only exception is the C5═N6 double bond, which is the least affected one by the basis set size in all CC methods. Similar qualitative and quantitative effects on bond lengths is seen when one goes from the 6 to 31G* to cc-pVDZ basis set within Møller−Plesset perturbation theory methods.

Increasing basis set size further, from cc-pVDZ to cc-pVTZ, makes all bonds shorter by about 0.015−0.020 Å within the coupled cluster ansatz. Again, however, bond shortening is considerably less for the C5═N6 bond (less than 0.012 Å). This is also the case for the ground-state geometries optimized at the MPn levels of theory. Due to the virtually constant impact of the basis set size on the bond lengths at discussed levels of theory, the bond length alternation (BLA, which is defined as the average length of the single bonds minus the average length of the double bonds) value is virtually not affected by the basis set size, as shown in Figure S3 of the Supporting Information.

Upgrading the basis set from 6-31G* to ANO-L-VDZP does have a relatively small effect on the bond lengths (up to 0.002 Å) resulting from CASSCF calculations. Increasing the basis set size further to triple-ζ, makes all bonds shorter by ca. 0.005 Å. This is reflected in essentially identical BLAs for 6-31G* and ANO-L-VTZP basis sets (Figure S3, Supporting Information).

For the CASPT2 approach, a difference between 6-31G* and ANO-L-VDZP bond lengths is more visible than in the case of CASSCF. For the ANO-L-VDZP basis set, each bond is longer by 0.005−0.010 Å. Increasing the basis set size to ANO-L-VTZP results in all bonds being shorter by by 0.008−0.014 Å. This corresponds to BLA values for CASPT2/6-31G* and CASPT2/ANO-L-VTZP geometries being in a very good agreement.

In the CASPT3 methodology, all bonds become 0.004−0.010 Å longer in ANO-L-VDZP than in the 6-31G* basis set. Expanding the basis set from ANO-L-VDZP to ANO-L-VTZP results in shortening of all bonds by 0.008−0.014 Å. This is in an excellent agreement with changes in geometrical properties when basis set size is increased for the CCSD and CCSD(T) optimization methods.

DOI: 10.1021/acs.jctc.6b00108
J. Chem. Theory Comput. 2016, 12, 2346−2356

Finally, increasing basis set size to quadruple-ζ when optimizing the ground-state geometry in CASSCF, CASPT2, CC2, and MP2 frameworks does not have a significant impact on the bond lengths compared to those obtained in the triple-ζ basis set. As it turns out, the 6-31G* basis set performs better than double-ζ with respect to the triple-ζ basis set in the case of CC, MPn, CASPT2, and CASPT3 geometry calculations.

3.2. Comparison of Ground-State Geometries Obtained from Different Methods Using Triple-ζ Basis Set. The CCSD(T)/cc-pVTZ method represents the highest level of theory approach for the geometry optimization discussed in this paper and can be considered as the reference one. In this subsection, discussion of the GS geometries obtained with various methods in the triple-ζ basis set relative to the CCSD(T)/cc-pVTZ is presented (Figure 2).

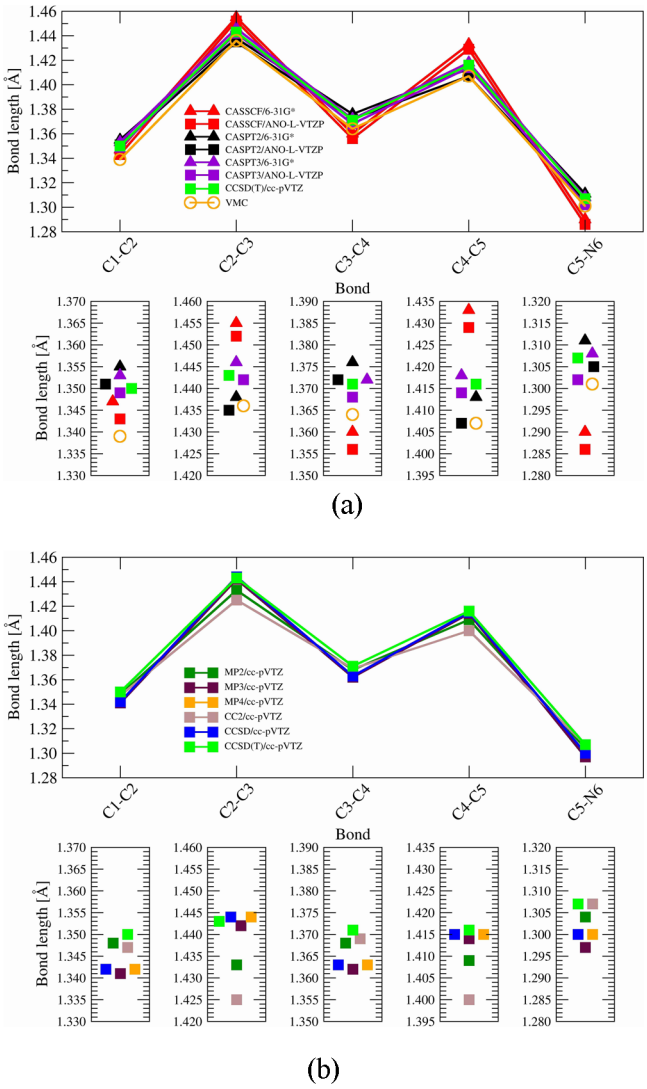

Figure 2. Bond lengths for the ground-state geometries obtained with various multireference (a) and single-reference (b) methods using triple-ζ basis sets (squares) and 6-31G* basis set (triangles). VMC (variational Monte Carlo) data are from ref 79. In panel (a) the bond lengths obtained with the reference CCSD(T)/cc-pVTZ method are also displayed. For numeration of atoms, see Figure 1. Under each panel, there is a plot showing an expansion of each bond length (the range in all cases is 0.040 Å; points were slightly moved apart for clarity).

As shown in Figure 2a, the CASSCF method gives overestimated single bond lengths by 0.009−0.013 Å and underestimated double bond lengths by 0.007−0.021 Å compared to the reference geometry. In fact, it is well known that not including dynamic correlation effects by the CASSCF methodology leads to overestimated single bond lengths and underestimated double bond lengths for larger RPSB models as well.[23−25,43,78]

CASPT2 double bond lengths are in an excellent agreement with the reference geometry, while single bonds are almost 0.010 Å shorter compared to the CCSD(T) structure. This is also the case for the MP2 geometry, which performs well due to the strong single-reference character of the ground-state wave function of retinal models in the equilibrium geometries. This is in an agreement with results for larger retinal models.[23−25]

CASPT3 offers great improvement in determining single bond lengths relative to the CASPT2 method. While double bond lengths, which were in excellent agreement with the reference values already at the CASPT2 level of theory, are virtually intact (with the exception of the C═N bond, which is 0.003 Å shorter for the CASPT3-based geometry), single bond lengths are improved significantly, by up to 0.007 Å, converging toward CCSD(T) values. In fact, CASPT3 results reveal that regardless of single and double CC bond characters, bond lengths diverge by no more than 0.003 Å from the reference values. This is in line with Werner's[58] study of a set of small diatomic molecules for which the CASPT3 equilibrium geometrical parameters are as accurate as the ones from MRCI and CCSD(T) when compared to experimental data. Surprisingly, our high-level CASPT3/ANO-L-VTZP and CCSD(T)/cc-pVTZ bond lengths differ from variational QMC data; a global shortening of all QMC bonds by almost 0.005−0.010 Å is seen (an even larger difference is obtained when QMC/cc-pVDZ or QMC/aug-cc-pVDZ results, which are very close to each other, are correlated with the CASPT3 and CCSD(T) ones in the double-ζ basis set; Figure S2, Supporting Information).[24,79] The same discrepancy between CCSD(T) and VMC structural parameters is also found for trans-1,3-butadiene.[80] On the other hand, VMC and CCSD(T) BLAs are exactly equal (Figure 3).

Interestingly, for the MP3 and MP4 geometries, single bond lengths are virtually the same as the reference ones, while double bond lengths are up to 0.010 Å shorter (Figure 2b). This is also the case for the CCSD geometry. On the other hand, the CC2 double bond lengths are in much better agreement with the CCSD(T) ones, while single bonds are ca. 0.017 Å shorter. This is reflected in the smallest BLA value among the investigated methods and, consequently, leads to the largest deviation from the CCSD(T) (0.015 Å difference) besides the CASSCF method (Figure 3).

Overall, the most successful method in reproducing the CCSD(T) reference geometry seems to be the CASPT3 method (maximum deviation in both CC bond lengths and BLA value is only 0.003 Å), while the poorest performance is obtained by the CASSCF method [for all basis sets, BLA's deviation is in the range of 0.023−0.025 Å (Figure S3, Supporting Information), whereas maximum deviation in bond lengths is as much as 0.020 Å (Figure S1, Supporting Information)], closely followed by CC2 (see above). However, other methods benchmarked in this paper and accounting for both static and dynamic electron correlations give either single (MP3, MP4, and CCSD) or double bond lengths (MP2,

DOI: 10.1021/acs.jctc.6b00108
J. Chem. Theory Comput. 2016, 12, 2346−2356

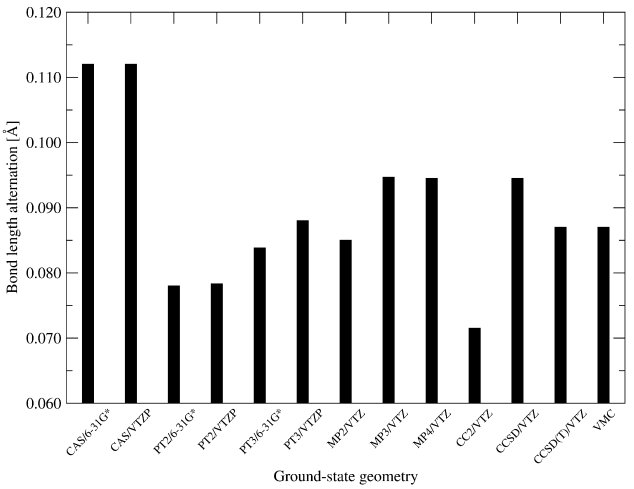

Figure 3. Bond length alternation (BLA) values for the ground-state geometries obtained with various methods in triple-ζ basis sets and with chosen methods in the 6-31G* basis set. VMC (variational Monte Carlo) value was taken from ref 79. The cc-pVTZ and ANO-L-VTZP basis set names are abbreviated as VTZ and VTZP, respectively. CASSCF, CASPT2, and CASPT3 methods names are abbreviated as CAS, PT2, and PT3, respectively.

CASPT2, and CC2) in an excellent agreement with the reference structure.

3.3. CASSCF, CASPT2, and CASPT3 Performance Using 6-31G* Basis Set. As explained in the Introduction, the CASPT2//CASSCF/6-31G* protocol seems to be intensively utilized in the investigation of the properties and processes related to retinals and retinylidene proteins. Moreover, sparse studies of the retinal's geometries in vacuo by the CASPT2 method are often limited to a rather small 6-31G* basis set, and as Walczak et al.[23] have shown for PSB5 models, such a basis set may be insufficient to capture certain geometrical features properly. Here, a comparison of geometrical parameters obtained at CASSCF, CASPT2, and CASPT3 levels of theory, using the 6-31G* basis set, with the ones from the reference CCSD(T)/cc-pVTZ method is presented (for bond lengths, see Figure 2; for BLAs, see Figure 3).

As shown in the previous subsection, if the source of the GS geometry is the CASSCF/ANO-L-VTZP and CCSD(T)/cc-pVTZ method, significant difference in bond lengths is observed. However, if one compares the CASSCF/6-31G* and CCSD(T)/cc-pVTZ geometries, there is a noticeable improvement in double bonds lengths when applying the 6-31G* basis set (by up to 0.004 Å), but at the same time, single bond lengths become slightly more divergent from the reference values (by up to 0.004 Å). A reverse trend is noticed when the CASPT2 method is utilized in the geometry optimization procedure instead of the CASSCF one. Unexpectedly, single C−C bond lengths obtained from CASPT2/6-31G* calculations are in better agreement with the CCSD(T)/cc-pVTZ data (by almost 0.005 Å) than the ones from CASPT2/ANO-L-VTZP calculations. On the other hand, double C═C bond lengths are improved by ca. 0.005 Å when the ANO-L-VTZP basis set is used. Consequently, the

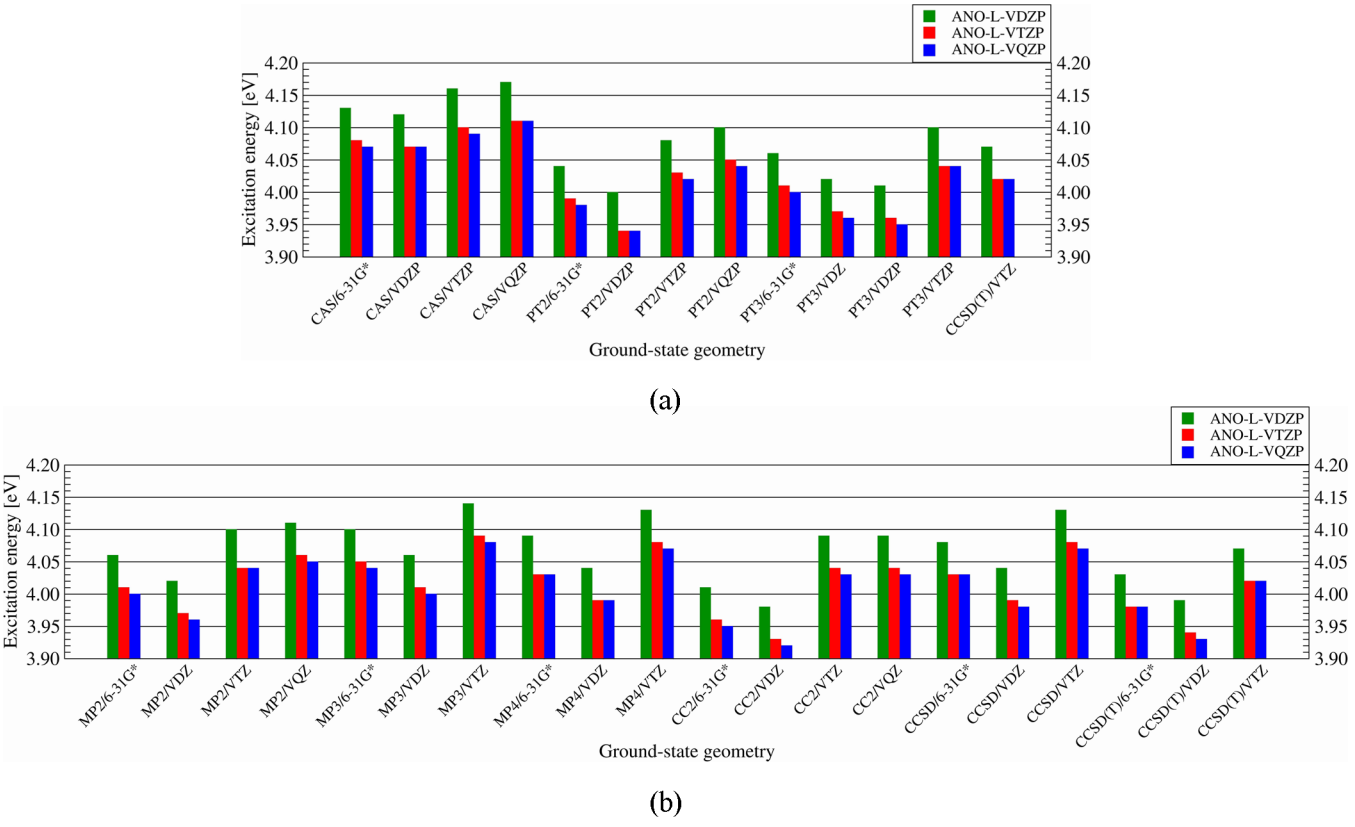

Figure 4. $S_0 \rightarrow S_1$ excitation energies calculated at SS-CASPT2/S-IPEA level of theory (ANO-L-VDZP, ANO-L-VTZP, and ANO-L-VQZP basis sets) utilizing ground-state molecular structures of the PSB3 model obtained at various multireference (a) and single-reference (b) levels of theory. In panel (a), results for the reference CCSD(T)/cc-pVTZ geometry are displayed. The cc-pVxZ and ANO-L-VxZP basis set names are abbreviated as VxZ and VxZP, respectively. CASSCF, CASPT2, and CASPT3 method names are abbreviated as CAS, PT2, and PT3, respectively.

DOI: 10.1021/acs.jctc.6b00108
J. Chem. Theory Comput. 2016, 12, 2346−2356

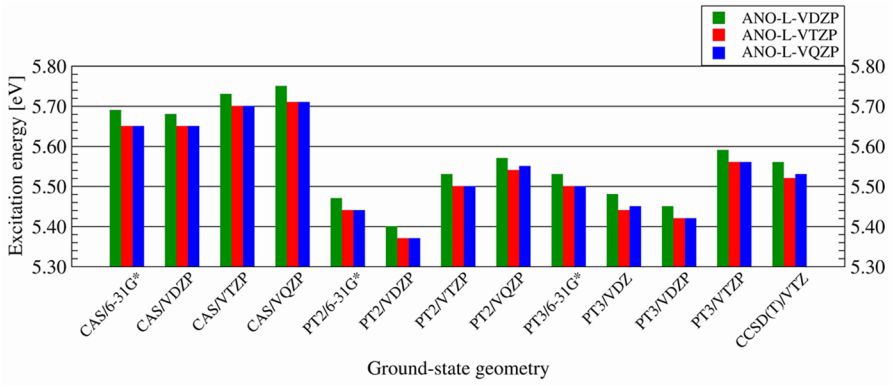

(a)

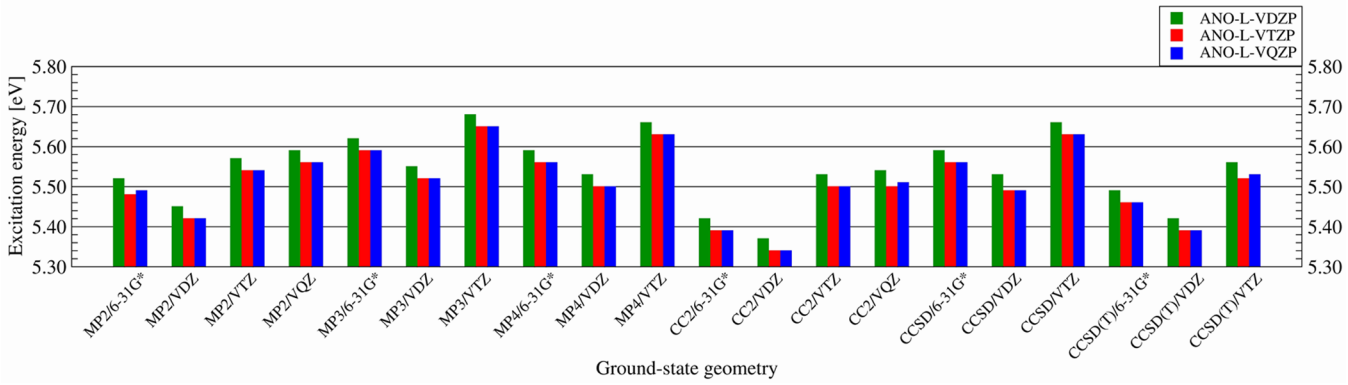

(b)

Figure 5. $S_0 \rightarrow S_2$ excitation energies calculated at SS-CASPT2/S-IPEA level of theory (ANO-L-VDZP, ANO-L-VTZP, and ANO-L-VQZP basis sets) utilizing ground-state molecular structures of the PSB3 model obtained at various multireference (a) and single-reference (b) levels of theory. In panel (a), results for the reference CCSD(T)/cc-pVTZ geometry are displayed. The cc-pVxZ and ANO-L-VxZP basis set names are abbreviated as VxZ and VxZP, respectively. CASSCF, CASPT2, and CASPT3 method names are abbreviated as CAS, PT2, and PT3, respectively.

CASPT2 geometries optimized in 6-31G* and ANO-L-VTZP basis sets give identical BLA, which is 0.009 Å smaller than in the case of the reference structure.

Third-order corrected equilibrium geometries of PSB3 have sligthtly improved single and double bonds lengths (by about 0.003 Å) over corresponding second-order corrected values when compared to the reference data. However, CASPT3-based bond lengths, contrary to the CASPT2 ones, are always exaggerated relative to the CCSD(T)/cc-pVTZ results, a deviation that further diminishes upon extension of the basis set to ANO-L-VTZP. Interestingly, reference values are always in between the CASPT3/6-31G* and CASPT3/ANO-L-VTZP ones.

One may thus conclude that the lowest-level of theory, the CASSCF/6-31G* method, presented here performs not very well in terms of bond lengths compared to significantly higher level of theory methods. Furthermore, it seems that increasing the basis set size from 6-31G* to ANO-L-VQZP in CASSCF geometry calculations provides no improvement in the quality of the equilibrium geometry. Within CASPT2 frameworks, 6-31G* to ANO-L-VTZP increment of basis set size does improve C═C and C═N double bond lengths but at the same time worsens single C−C bond lengths. At the CASPT3 levels of theory, the 6-31G* basis set is as reliable as the much larger ANO-L-VTZP basis set in reproducing reference geometry.

4. EXCITATION ENERGIES

4.1. Impacts of Geometry on Excitation Energies. In this subsection, the effect of the methodology (along with the basis set effect) selected to perform the ground-state geometry optimization on the excitation energies is shown (for bond lengths, see Figure 2 and Figures S1 and S2, Supporting Information). For excitation energies calculated at the CASPT2 level of theory, see Figures 4 and 5 and Tables S1−S4 of the Supporting Information.

Basis Set Effect. At all presented coupled cluster levels of theory, going from 6-31G* to cc-pVDZ basis sets in the geometry optimization procedure lowers the $S_0 \rightarrow S_1$ excitation energy by about 0.05 eV. Similarly, the $S_0 \rightarrow S_2$ excitation energy (EE) decreases, but this effect is a bit larger (0.05−0.07 eV). As was already indicated, the discussed basis set size impact on geometrical features is virtually the same for the Møller−Plesset perturbation theory methods; thus, this is also the case for energetic properties. Excitation energies to both lowest-lying singlet states are considerably larger when the cc-pVTZ instead of cc-pVDZ basis set is used for geometry optimization with MP and CC methods. This effect is ca. 0.10 and 0.15 eV for the $S_0 \rightarrow S_1$ and $S_0 \rightarrow S_2$ transitions, respectively.

In the case of the CASSCF/6-31G* and CASSCF/ANO-L-VDZP GS geometries, the EEs are virtually the same. Increasing basis set size in the GS geometry optimization procedure to VTZP makes the transition energy for both states larger by up to 0.05 eV.

DOI: 10.1021/acs.jctc.6b00108
J. Chem. Theory Comput. 2016, 12, 2346−2356

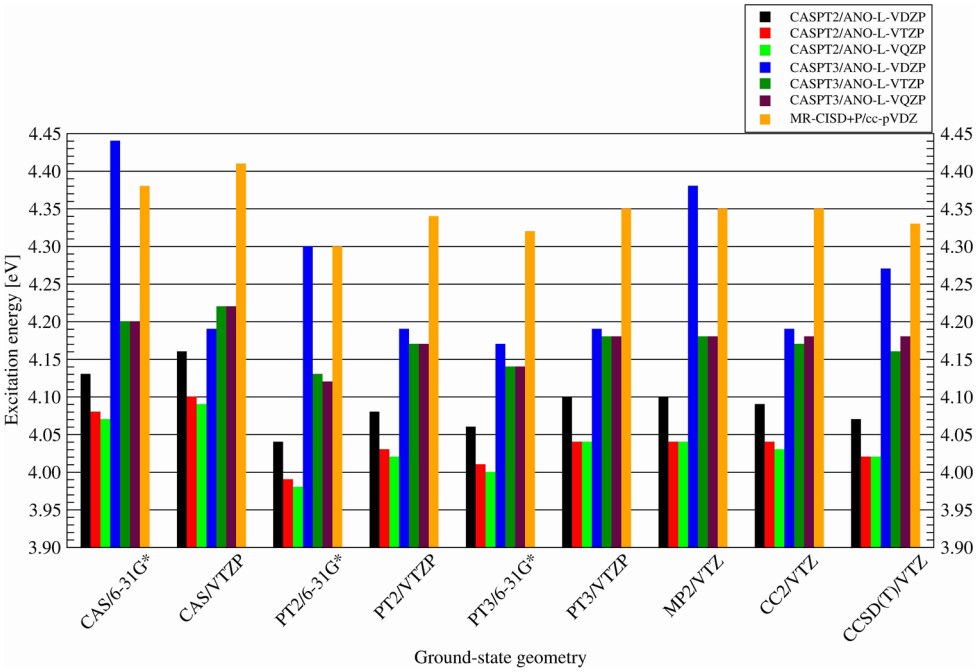

Figure 6. $S_0 \rightarrow S_1$ excitation energies calculated with SS-CASPT2/S-IPEA and CASPT3/S-IPEA methods in ANO-L-VDZP, ANO-L-VTZP, and ANO-L-VQZP basis sets. MR-CISD/cc-pVDZ including Pople correction results are also displayed. Calculations were performed for the ground-state geometries of the PSB3 model obtained with various methods in triple-ζ basis sets and with chosen methods in the 6-31G* basis set. The cc-pVTZ and ANO-L-VTZP basis set names are abbreviated as VTZ and VTZP, respectively. CASSCF, CASPT2, and CASPT3 method names are abbreviated as CAS, PT2, and PT3, respectively.

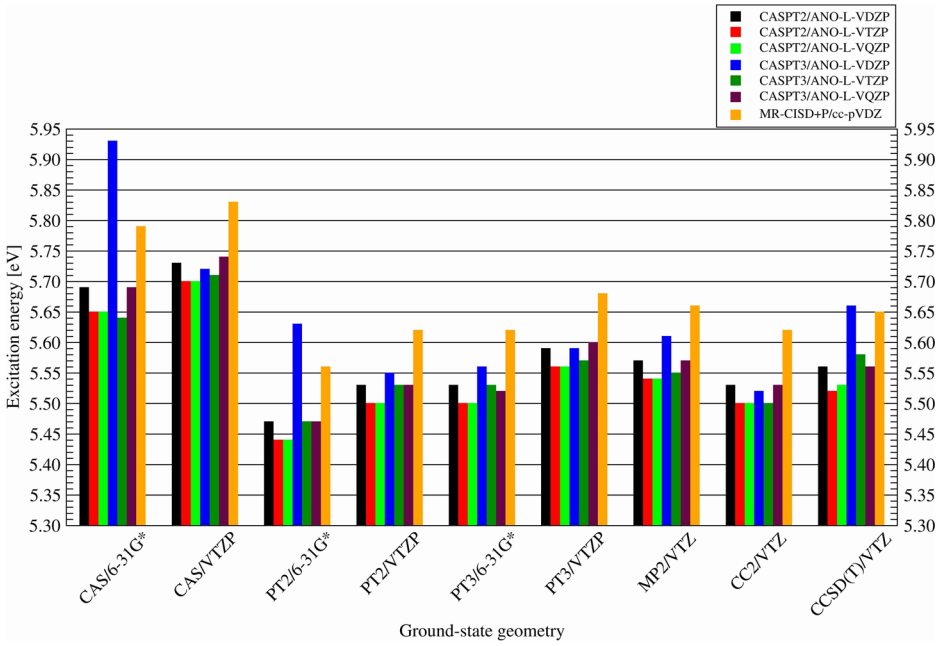

Figure 7. $S_0 \rightarrow S_2$ excitation energies calculated with SS-CASPT2/S-IPEA and CASPT3/S-IPEA methods in ANO-L-VDZP, ANO-L-VTZP, and ANO-L-VQZP basis sets. MR-CISD/cc-pVDZ including Pople correction results are also displayed. Calculations were performed for the ground-state geometries of the PSB3 model obtained with various methods in triple-ζ basis sets and with chosen methods in the 6-31G* basis set. The cc-pVTZ and ANO-L-VTZP basis set names are abbreviated as VTZ and VTZP, respectively. CASSCF, CASPT2, and CASPT3 method names are abbreviated as CAS, PT2, and PT3, respectively.

Compared to the CASPT2/6-31G* geometry, the CASPT2/ANO-L-VDZP structure makes the $S_0 \rightarrow S_1$ and $S_0 \rightarrow S_2$ EEs lower by ca. 0.05 and 0.07 eV, respectively. Upon expansion of the basis set size to ANO-L-VTZP, the transition energies to S_1 and S_2 increase by 0.08−0.13 eV.

In the CASPT3 methodology, the $S_0 \rightarrow S_1$ and $S_0 \rightarrow S_2$ EEs are 0.05−0.08 eV lower when optimization was performed in the ANO-L-VDZP basis set instead of the 6-31G* basis set. The excitation energies for the S_1 and S_2 states raise by ca. 0.10 and 0.15 eV, respectively, when the basis set size is increased to ANO-L-VTZP. This is in excellent agreement with changes in

DOI: 10.1021/acs.jctc.6b00108
J. Chem. Theory Comput. 2016, 12, 2346−2356

both energetic and geometric properties when basis set size is increased at the CCSD(T) level of theory.

Methodology Assessment. Comparison of excitation energies (CASPT2/ANO-L-VQZP) obtained for PSB3 models optimized by different methods in triple-ζ basis sets reveals that the excitation energies range from 4.02 to 4.09 eV for the $S_0 \rightarrow S_1$ transition and 5.50 to 5.70 eV for the $S_0 \rightarrow S_2$ transition (Figures 4 and 5 and Tables S1−S2, Supporting Information). In each case, the CASSCF/ANO-L-VTZP-based geometry provides the highest excitation energy, while CASPT2/ANO-L-VTZP provides the lowest one.

A rather poor quality of the CASSCF/ANO-L-VTZP geometry is manifested in EEs. Excitation energies for S_1 and S_2 states, based on the CASSCF/ANO-L-VTZP geometry, are overestimated by 0.07 and 0.17 eV, respectively, when compared to the corresponding values calculated for the reference geometry. The CASSCF/6-31G* geometry does a better job decreasing the above-mentioned deviations to 0.05 and 0.12 eV, respectively. For MP3, MP4, and CCSD geometries, which yield very good quality single bond lengths, the excitation energies to both discussed states are overestimated by 0.05−0.12 eV compared to the corresponding values calculated for the reference CCSD(T)/cc-pVTZ geometry (Figures 4 and 5). In case of the CASPT2, MP2, CC2, and CCSD(T) geometries, the agreement is very good for both transitions (up to ±0.03 eV) and corresponds to an excellent agreement in double bond lengths as has already been discussed. Notice that even though the CC2 method falls short to reproduce the reference single bond lengths, it does a great job in describing electronic transitions to the two lowest excited states. Furthermore, the best performance of CASPT3 in terms of geometry optimization with respect to the CCSD(T) geometry and truly balanced description of both single and double bonds is not mirrored in any improvement of already excellent EEs derived for CASPT2, MP2, or CC2 geometries.

4.2. Comparison of CASPT2 and CASPT3 Excitation Energies. In this subsection, the excitation energies to the two lowest singlet excited states obtained using the CASPT2 method are assessed by comparison with CASPT3 results (Figures 6 and 7 and Tables S1, S2, S5, and S6, Supporting Information). Such calculations were performed for the reference CCSD(T) geometry along with CASPT3, CASPT2, CASSCF, MP2, and CC2 geometries optimized in the triple-ζ basis set. Additionally, for CASSCF, CASPT2, and CASPT3 geometries optimized in the 6-31G* basis set, such comparison was also put forward. The multireference perturbation theory methods recover both dynamic and static electron correlation, but they do not belong to black box approaches. Thus, the choice of the complete active space size and various parameters influence the results. In this study, we focus on investigating the basis set effect as well as the choice of the zeroth-order Hamiltonian (IPEA shift parameter utilized) on the resulting excitation energies (see Tables S1, S2, and S7−S9, Supporting Information).

Basis Set Effect. It comes as no surprise that the choice of the basis set utilized in CASPT2 and CASPT3 excitation energy calculations does influence to some extent excitation energies (Figures 6 and 7 and Tables S1, S2, S5, and S6, Supporting Information). The CASPT2/ANO-L-VTZP EEs are ca. 0.05 eV lower than the CASPT2/ANO-L-VDZP ones. Increasing the basis set size to quadruple-ζ has an effect no greater than 0.01 eV compared to the ANO-L-VTZP results. This is consistent with results obtained by Valsson et al.[24]

The basis set effect is more pronounced in CASPT3 calculations. CASPT3/ANO-L-VTZP EEs to the two lowest excited states are within 4.13−4.22 and 5.47−5.71 eV, respectively (for geometries obtained using the 6-31G* and ANO-L-VTZP basis sets, see Tables S5 and S6, Supporting Information). The corresponding CASPT3/ANO-L-VDZP results are 4.17−4.44 and 5.52−5.93 eV, respectively. First, the basis set effect does not generate a constant shift as it varies between 0.01−0.24 eV for the $S_0 \rightarrow S_1$ transition and 0.01−0.29 eV for the $S_0 \rightarrow S_2$ transition, depending strongly on the geometry. Second, increasing the number of basis functions does not always downshift the excitation energies. In fact, for the CASSCF/ANO-L-VTZP geometry, the $S_0 \rightarrow S_1$ excitation energy is greater in ANO-L-VTZP than in the ANO-L-VDZP basis set. Increasing the basis set from ANO-L-VTZP to ANO-L-VQZP has a non-negligible effect on the excitation energies, shifting them in a range of −0.02 to 0.05 eV.

In light of the presented results, we may conclude that CASPT3-based excitation energies are more sensitive to the basis set size than CASPT2 ones. While for the latter method a triple-ζ quality basis set seems to be sufficient to describe the excitation energies to the lowest-lying states, it is not the case for the former method for which a quadruple-ζ or even more extensive basis set is required.

IPEA Shift Effect. We have also investigated the impact of the modification of the zeroth-order Hamiltonian (IPEA shift parameter) on the resulting CASPT2 and CASPT3 excitation energies since it is well known to influence dramatically CASPT2 excitation energies. The IPEA parameter was introduced because the CASPT2 protocol tends to overestimate the correlation energy of the excited state leading to underestimated excitation energies values. The IPEA shift is a correction to the zeroth-order Hamiltonian which changes the orbital energies so that they become closer to the ionization energies when excited from and closer to the electronic affinities when excited to.[48] In the present CASPT2 calculations, the $S_0 \rightarrow S_1$ and $S_0 \rightarrow S_2$ excitation energies obtained with S-IPEA are on average 0.35 and 0.40 eV greater compared to the 0-IPEA results, respectively (Tables S1−S2, Supporting Information). This is in agreement with results reported for PSB3 and methylated PSB3 models[24,25,55] as well as PSB5 models.[23]

On the contrary, the IPEA shift has a much smaller effect on third-order energies (Table S7, Supporting Information), supporting Werner's finding.[58] In particular, $S_0 \rightarrow S_1$ excitation energies are changed by 0.01−0.02 eV upon modifying the Hamiltonian (Table S7, Supporting Information).[81] A detailed insight into CASPT3 results reveals that, similarly to CASPT2, a difference in the excitation energies calculated with or without introduction of the IPEA shift parameter is essentially constant for all the geometries studied here (Tables S1−S4, Supporting Information).

CASPT2 vs CASPT3 in ANO-L-VQZP Basis Set. For each GS geometry discussed here, the CASPT3/ANO-L-VQZP EEs for the S_1 state are higher by 0.13−0.16 eV than their CASPT2/ANO-L-VQZP counterparts (Figure 6 and Tables S1 and S5, Supporting Information). It appears that third-order results do have a less visible impact on the $S_0 \rightarrow S_2$ EEs (Figure 7 and Tables S2 and S6, Supporting Information). Specifically, for all PSB3 geometries studied here, a third-order correction adds 0.02−0.04 eV relative to the CASPT2 energies. Third-order EEs to the S_2 electronic state are more strongly dependent on

DOI: 10.1021/acs.jctc.6b00108
J. Chem. Theory Comput. 2016, 12, 2346−2356

the geometry than EEs to the S_1 state spanning the wider range of energies—0.27 eV vs 0.10 eV, respectively.

The magnitude of the CASPT3-CASPT2 (in ANO-L-VQZP basis set) EEs shifts for the reference CCSD(T)/cc-pVTZ geometry is 0.16 and 0.03 eV for the $S_0 \rightarrow S_1$ and $S_0 \rightarrow S_2$ transitions, respectively, and is very similar to the CASPT3/ANO-L-VTZP geometry (0.14 and 0.04 eV) and other geometries as well. One needs to be aware that CASPT3 results are not completely consistent due to basis set incompletness, uncorrelated core−valence electrons, and limited reference space. CASPT3 excitation energies converge toward MR-CISD+Q (with Pople correction) (Figures 6 and 7; compare data in Tables S5−S6 and Tables S10−S11, Supporting Information). In fact, the $S_0 \rightarrow S_1$ energies are within ca. 0.18 eV and the $S_0 \rightarrow S_2$ ones are within ca. 0.10 eV. The larger deviation for the excitation to the lower-energy excited state is in line with the finding that for states with more diffused charge (e.g., S_1 ionic state compared to the S_2 covalent one) the discrepancy between CASPT2 and MR-CISD energies is larger. Indeed, it also holds true for CASPT3 results. We also note that the CASPT3/ANO-L-VQZP method yields the $S_0 \rightarrow S_1$ excitation energy (4.18 eV for the CCSD(T) geometry) in close agreement with the diffusion QMC/cc-pVQZ result (4.22(2) eV for B3LYP geometry) by Valsson and Filippi.[24] A variational QMC/cc-pVQZ energy by the same authors is 0.16 eV higher than our CASPT3 data.

5. CONCLUSIONS

Extensive evaluation of the performance of various single-reference and multireference ab initio methods in terms of the ground-state geometry of the minimal model of retinal (PSB3) and its impact on the excitation energies to the two lowest excited states is presented here. Obtained geometries are assessed relative to the CCSD(T)/cc-pVTZ geometry, while calculated excitation energies with respect to CASPT3/ANO-L-VQZP values. To the best of our knowledge, this is the very first study to report CASPT3 ground-state geometries and vertical excitation energies of retinal models.

To summarize, one may see that the methods benchmarked in this paper give either single (MP3, MP4, and CCSD) or double bond lengths (MP2, CASPT2, and CC2) in excellent agreement with the CCSD(T)/cc-pVTZ reference structure. What is interesting is that the excitation energies for the geometries from the latter group of methods are in a better agreement with the corresponding energies calculated for the reference structure. However, CASPT3/ANO-L-VTZP is the only method among those investigated here that provides all bond lengths in almost perfect correspondence with the reference structure. This is reflected in very close CASPT3/ANO-L-VQZP excitation energies for CCSD(T) and CASPT3 geometries in the triple-ζ basis set. One should also notice a better performance of the CC2/cc-pVTZ method than the CCSD/cc-pVTZ method in terms of bond lengths and energetic properties.

It comes as no surprise that CASSCF geometries deviate significantly from the CCSD(T) reference data. Nevertheless, this structural discrepancy does not have a significant effect on the energetic properties of the bright state as the $S_0 \rightarrow S_1$ CASPT2- and CASPT3-based excitation energies do not deviate by more than 0.07 eV from the corresponding values calculated for the reference structure. The structural defects of the CASSCF geometry do manifest themselves more strongly in the $S_0 \rightarrow S_2$ excitation energies which are ca. 0.18 eV overestimated. The larger the basis set is, the less accurate EEs are obtained.

Third-order corrected (CASPT3) excitation energies to the S_1 and S_2 electronic states are on average 0.14 and 0.03 eV, respectively, higher than their CASPT2 counterparts. Moreover, the CASPT3 method is much less sensitive to modifications of the effective Hamiltonian (IPEA shift) than the CASPT2 one. In the former method, the changes in the EEs upon introducing the IPEA shift parameter are 0.01−0.02 eV compared to 0.30−0.40 eV values in case of the latter method. However, CASPT3 seems to be more basis set size dependent, and one needs to use a quadruple-ζ or even more extensive basis sets to obtain sufficiently converged results.

To conclude, we believe that the CASPT3 results discussed here provide reliable benchmarks to assess the accuracy of CASPT2//CASSCF- and CASPT2-based excitation energies of minimal retinal models, which can be utilized for further investigations of retinals both in vacuo as well as in the protein environment.

■ ASSOCIATED CONTENT

Supporting Information

The Supporting Information is available free of charge on the ACS Publications website at DOI: 10.1021/acs.jctc.6b00108.

Plots of bond lengths for geometries obtained using various computational methods; bond length alternation values for all geometries studied here; plots of SS-CASPT2 and MR-CISD excitation energies; exemplary natural orbitals creating the active space; plots of average sum of the Mulliken charges calculated with SS-CASPT2 methods; dipole moment changes upon excitation calculated with SS-CASPT2 and MR-CISD methods; tables with excitation energies, oscillator strengths, and dipole moment changes calculated with the CASPT2 method utilizing various basis sets, CASSCF reference wave functions, IPEA parameter values, and either single-state or multistate protocol; tables with excitation energies, oscillator strengths, and dipole moment changes calculated with MR-CISD method and including Davidson or Pople corrections (not for dipole moment changes); tables with excitation energies and oscillator strengths calculated with the CASPT3 method for various basis sets; tables with excitation energies calculated with the CASPT3 method for various IPEA parameter values; Cartesian coordinates and absolute energy values for the ground-state geometries discussed here. (PDF)

■ AUTHOR INFORMATION

Corresponding Author

*E-mail: tadeusz.andruniow@pwr.wroc.pl.

Notes

The authors declare no competing financial interest.

■ ACKNOWLEDGMENTS

We acknowledge a statutory activity subsidy from the Polish Ministry of Science and Higher Education for the Faculty of Chemistry of Wroclaw University of Technology. This work was financed by Wroclaw Research Centre EIT+ under the project BIOMED "Biotechnologies and advanced medical technologies" (POIG 01.01.02-02-003/08) financed from European Development Fund Operational Programme In-

DOI: 10.1021/acs.jctc.6b00108
J. Chem. Theory Comput. 2016, 12, 2346−2356

novative Economy 1.1.2. Calculations were performed at the Wroclaw Supercomputer and Networking Center (WCSS) and Academic Computer Center Cyfronet AGH in Krakow.

REFERENCES

(1) Spudich, J. L.; Yang, C.-S.; Jung, K.-H.; Spudich, E. N. *Annu. Rev. Cell Dev. Biol.* **2000**, *16*, 365−392.
(2) Spudich, J. L., Jung, K.-H. Microbial Rhodopsins: Phylogenetic and Functinal Diversity. In *Handbook of Photosensory Receptors*; Briggs, W. R., Spundich, J. L., Eds.; Wiley-VCH: Weinheim, Germany, 2005; pp 1−23.
(3) Ernst, O. P.; Lodowski, D. T.; Elstner, M.; Hegemann, P.; Brown, L. S.; Kandori, H. *Chem. Rev.* **2014**, *114*, 126−163.
(4) Haran, G.; Morlino, E. A.; Matthes, J.; Callender, R. H.; Hochstrasser, R. M. *J. Phys. Chem. A* **1999**, *103*, 2202−2207.
(5) Kandori, H.; Furutani, Y.; Nishimura, S.; Shichida, Y.; Chosrowjan, H.; Shibata, Y.; Mataga, N. *Chem. Phys. Lett.* **2001**, *334*, 271−276.
(6) Polli, D.; Altoè, P.; Weingart, O.; Spillane, K. M.; Manzoni, C.; Brida, D.; Tomasello, G.; Orlandi, G.; Kukura, P.; Mathies, R. A.; Garavelli, M.; Cerullo, G. *Nature* **2010**, *467*, 440−443.
(7) Tittor, J.; Oesterhelt, D. *FEBS Lett.* **1990**, *263*, 269−273.
(8) Kim, J. E.; Tauber, M. J.; Mathies, R. A. *Biochemistry* **2001**, *40*, 13774−13778.
(9) Grote, M.; O'Malley, M. A. *FEMS Microbiol. Rev.* **2011**, *35*, 1082−1089.
(10) Koyanagi, M.; Terakita, A. *Biochim. Biophys. Acta, Bioenerg.* **2014**, *1837*, 710−716.
(11) Rivado-Casas, L.; Sampedro, D.; Campos, P. J.; Fusi, S.; Zanirato, V.; Olivucci, M. J. *J. Org. Chem.* **2009**, *74*, 4666−4674.
(12) Lumento, F.; Zanirato, V.; Fusi, S.; Busi, E.; Latterini, L.; Elisei, F.; Sinicropi, A.; Andruniów, T.; Ferré, N.; Basosi, R.; Olivucci, M. *Angew. Chem., Int. Ed.* **2007**, *46*, 414−420.
(13) Hendrickx, E.; Clays, K. J.; Persoons, A. P.; Dehu, C.; Brédas, J. L. *J. Am. Chem. Soc.* **1995**, *117*, 3547−3555.
(14) Kandori, H.; Shichida, Y.; Yoshizawa, T. *Biochemistry (Moscow)* **2001**, *66*, 1197−1209.
(15) Kukura, P.; McCamant, D. W.; Yoon, S.; Wandschmeider, D. B.; Mathies, R. A. *Science* **2005**, *310*, 1006−1009.
(16) Meyer, C. K.; Böhme, M.; Ockenfels, A.; Gärtner, W.; Hofmann, K. P.; Ernst, O. P. *J. Biol. Chem.* **2000**, *275*, 19713−19718.
(17) Patel, A. B.; Crocker, E.; Eilers, M.; Hirshfeld, A.; Sheves, M.; Smith, S. O. *Proc. Natl. Acad. Sci. U. S. A.* **2004**, *101*, 10048−10053.
(18) Kennis, J. T. M.; Groot, M.-L. *Curr. Opin. Struct. Biol.* **2007**, *17*, 623−630.
(19) McCamant, D. W.; Kukura, P.; Mathies, R. A. *J. Phys. Chem. B* **2005**, *109*, 10449−10457.
(20) Herbst, J.; Heyne, K.; Diller, R. *Science* **2002**, *297*, 822−825.
(21) Kobayashi, T.; Saito, T.; Ohtani, H. *Nature* **2001**, *414*, 531−534.
(22) Møller, C.; Plesset, M. S. *Phys. Rev.* **1934**, *46*, 618−622.
(23) Walczak, E.; Szefczyk, B.; Andruniów, T. *J. Chem. Theory Comput.* **2013**, *9*, 4915−4927.
(24) Valsson, O.; Filippi, C. *J. Chem. Theory Comput.* **2010**, *6*, 1275−1292.
(25) Valsson, O.; Angeli, C.; Filippi, C. *Phys. Chem. Chem. Phys.* **2012**, *14*, 11015−11020.
(26) Garavelli, M.; Celani, P.; Bernardi, F.; Robb, M. A.; Olivucci, M. *J. Am. Chem. Soc.* **1997**, *119*, 6891−6901.
(27) Garavelli, M.; Bernardi, F.; Olivucci, M.; Vreven, T.; Klein, S.; Celani, P.; Robb, M. A. *Faraday Discuss.* **1998**, *110*, 51−70.
(28) Garavelli, M.; Vreven, T.; Celani, P.; Bernardi, F.; Robb, M. A.; Olivucci, M. *J. Am. Chem. Soc.* **1998**, *120*, 1285−1288.
(29) González-Luque, R.; Garavelli, M.; Bernardi, F.; Merchan, M.; Robb, M. A.; Olivucci, M. *Proc. Natl. Acad. Sci. U. S. A.* **2000**, *97*, 9379−9384.
(30) De Vico, L.; Page, C. S.; Garavelli, M.; Bernardi, F.; Basosi, R.; Olivucci, M. *J. Am. Chem. Soc.* **2002**, *124*, 4124−4134.
(31) Cembran, A.; Bernardi, F.; Olivucci, M.; Garavelli, M. *J. Am. Chem. Soc.* **2003**, *125*, 12509−12519.
(32) De Vico, L.; Garavelli, M.; Bernardi, F.; Olivucci, M. *J. Am. Chem. Soc.* **2005**, *127*, 2433−2442.
(33) Cembran, A.; González-Luque, R.; Altoè, P.; Merchán, M.; Bernardi, F.; Olivucci, M.; Garavelli, M. *J. Phys. Chem. A* **2005**, *109*, 6597−6605.
(34) Fantacci, S.; Migani, A.; Olivucci, M. *J. Phys. Chem. A* **2004**, *108*, 1208−1213.
(35) Ferré, N.; Olivucci, M. *J. Am. Chem. Soc.* **2003**, *125*, 6868−6869.
(36) Andruniów, T.; Ferré, N.; Olivucci, M. *Proc. Natl. Acad. Sci. U. S. A.* **2004**, *101*, 17908−17913.
(37) Frutos, L. M.; Andruniów, T.; Santoro, F.; Ferré, N.; Olivucci, M. *Proc. Natl. Acad. Sci. U. S. A.* **2007**, *104*, 7764−7769.
(38) Ferré, N.; Cembran, A.; Garavelli, M.; Olivucci, M. *Theor. Chem. Acc.* **2004**, *112*, 335−341.
(39) Tomasello, G.; Olaso-González, G.; Altoè, P.; Stenta, M.; Serrano-Andrés, L.; Merchán, M.; Orlandi, G.; Bottoni, A.; Garavelli, M. *J. Am. Chem. Soc.* **2009**, *131*, 5172−5186.
(40) Roos, B. O.; Taylor, P. R.; Siegbahn, P. E. M. *Chem. Phys.* **1980**, *48*, 157−173.
(41) Andersson, K.; Malmqvist, P.-Å; Roos, B. O. *J. Chem. Phys.* **1992**, *96*, 1218−1226.
(42) Schapiro, I.; Ryazantsev, M. N.; Ding, W. J.; Huntress, M. M.; Melaccio, F.; Andruniów, T.; Olivucci, M. *Aust. J. Chem.* **2010**, *63*, 413−429.
(43) Page, C. S.; Olivucci, M. *J. Comput. Chem.* **2003**, *24*, 298−309.
(44) Christiansen, O.; Koch, H.; Jørgensen, P. *Chem. Phys. Lett.* **1995**, *243*, 409−418.
(45) Bartlett, R. J. *J. Phys. Chem.* **1989**, *93*, 1697−1708.
(46) Gozem, S.; Huntress, M.; Schapiro, I.; Lindh, R.; Granovsky, A. A.; Angeli, C.; Olivucci, M. *J. Chem. Theory Comput.* **2012**, *8*, 4069−4080.
(47) Analytic gradients are available for CASPT2 calculations in Molpro 2012.1[65] but only for molecular systems with limited number of correlated orbitals, up to 32 for machines with 64-bit integers.
(48) Ghigo, G.; Roos, B. O.; Malmqvist, P.-Å. *Chem. Phys. Lett.* **2004**, *396*, 142−149.
(49) Send, R.; Sundholm, D. *J. Phys. Chem. A* **2007**, *111*, 27−33.
(50) Send, R.; Sundholm, D. *J. Phys. Chem. A* **2007**, *111*, 8766−8773.
(51) Send, R.; Sundholm, D. *J. Mol. Model.* **2008**, *14*, 717−726.
(52) Send, R.; Sundholm, D.; Johansson, M. P.; Pawłowski, F. *J. Chem. Theory Comput.* **2009**, *5*, 2401−2414.
(53) Tuna, D.; Lefrancois, D.; Wolański, Ł.; Gozem, S.; Schapiro, I.; Andruniów, T.; Dreuw, A.; Olivucci, M. *J. Chem. Theory Comput.* **2015**, *11*, 5758−5781.
(54) Keal, T. W.; Wanko, M.; Thiel, W. *Theor. Chem. Acc.* **2009**, *123*, 145−156.
(55) Gozem, S.; Melaccio, F.; Lindh, R.; Krylov, A. I.; Granovsky, A. A.; Angeli, C.; Olivucci, M. *J. Chem. Theory Comput.* **2013**, *9*, 4495−4506.
(56) Rivalta, I.; Nenov, A.; Garavelli, M. *Phys. Chem. Chem. Phys.* **2014**, *16*, 16865−16879.
(57) Szymczak, J. J.; Barbatti, M.; Lischka, H. *J. Chem. Theory Comput.* **2008**, *4*, 1189−1199.
(58) Werner, H.-J. *Mol. Phys.* **1996**, *89*, 645−661.
(59) Kerkines, I.; Ćarsky, P.; Mavridis, A. *J. Phys. Chem. A* **2005**, *109*, 10148−10152.
(60) Gu, J.; Lin, Y.; Wu, W.; Shaik, S.; Ma, B. *J. Chem. Theory Comput.* **2008**, *4*, 2101−2107.
(61) Takatani, T.; Sears, J.; Sherrill, C. *J. Phys. Chem. A* **2010**, *114*, 11714−11718.
(62) Woywod, C.; Papp, A.; Halász, J.; Vibók, A. *Theor. Chem. Acc.* **2010**, *125*, 521−533.
(63) Schild, A.; Paulus, B. *J. Comput. Chem.* **2013**, *34*, 1393−1397.
(64) Aquilante, F.; De Vico, L.; Ferré, N.; Ghigo, G.; Malmqvist, P.-Å; Neogrády, P.; Pedersen, T. B.; Pitoňák, M.; Reiher, M.; Roos, B. O.; Serrano-Andrés, L.; Urban, M.; Veryazov, V.; Lindh, R. *J. Comput. Chem.* **2010**, *31*, 224−247.

DOI: 10.1021/acs.jctc.6b00108
J. Chem. Theory Comput. 2016, 12, 2346−2356

(65) Werner, H.-J.; Knowles, P. J.; Knizia, G.; Manby, F. R.; Schütz, M.; Celani, P.; Korona, T.; Lindh, R.; Mitrushenkov, A.; Rauhut, G.; Shamasundar, K. R.; Adler, T. B.; Amos, R. D.; Bernhardsson, A.; Berning, A.; Cooper, D. L.; Deegan, M. J. O.; Dobbyn, A. J.; Eckert, F.; Goll, E.; Hampel, C.; Hesselmann, A.; Hetzer, G.; Hrenar, T.; Jansen, G.; Köppl, C.; Liu, Y.; Lloyd, A. W.; Mata, R. A.; May, A. J.; McNicholas, S. J.; Meyer, W.; Mura, M. E.; Nicklass, A.; O'Neill, D. P.; Palmieri, P.; Pflüger, K.; Pitzer, R.; Reiher, M.; Shiozaki, T.; Stoll, H.; Stone, A. J.; Tarroni, R.; Thorsteinsson, T.; Wang, M.; Wolf, A. *MOLPRO*, version 2012.1, a package of ab initio programs. http://www.molpro.net (accessed April 2016).
(66) Ditchfield, R.; Hehre, W. J.; Pople, J. A. *J. Chem. Phys.* **1971**, *54*, 724−726.
(67) Widmark, P.-O.; Malmqvist, P.-Å.; Roos, B. O. *Theor. Chem. Acta* **1990**, *77*, 291−306.
(68) Widmark, P.-O.; Persson, B. J.; Roos, B. O. *Theor. Chim. Acta* **1991**, *79*, 419−432.
(69) Pou-AméRigo, R.; Merchán, M.; Nebot-Gil, I.; Widmark, P.-O.; Roos, B. O. *Theor. Chim. Acta* **1995**, *92*, 149−181.
(70) Frisch, M. J.; Trucks, G. W.; Schlegel, H. B.; Scuseria, G. E.; Robb, M. A.; Cheeseman, J. R.; Scalmani, G.; Barone, V.; Mennucci, B.; Petersson, G. A.; Nakatsuji, H.; Caricato, M.; Li, X.; Hratchian, H. P.; Izmaylov, A. F.; Bloino, J.; Zheng, G.; Sonnenberg, J. L.; Hada, M.; Ehara, M.; Toyota, K.; Fukuda, R.; Hasegawa, J.; Ishida, M.; Nakajima, T.; Honda, Y.; Kitao, O.; Nakai, H.; Vreven, T.; Montgomery, J. A., Jr.; Peralta, J. E.; Ogliaro, F.; Bearpark, M.; Heyd, J. J.; Brothers, E.; Kudin, K. N.; Staroverov, V. N.; Kobayashi, R.; Normand, J.; Raghavachari, K.; Rendell, A.; Burant, J. C.; Iyengar, S. S.; Tomasi, J.; Cossi, M.; Rega, N.; Millam, J. M.; Klene, M.; Knox, J. E.; Cross, J. B.; Bakken, V.; Adamo, C.; Jaramillo, J.; Gomperts, R.; Stratmann, R. E.; Yazyev, O.; Austin, A. J.; Cammi, R.; Pomelli, C.; Ochterski, J. W.; Martin, R. L.; Morokuma, K.; Zakrzewski, V. G.; Voth, G. A.; Salvador, P.; Dannenberg, J. J.; Dapprich, S.; Daniels, A. D.; Farkas, Foresman, J. B.; Ortiz, J. V.; Cioslowski, J.; Fox, D. J. *Gaussian 09*, Revision D.01 Gaussian, Inc.: Wallingford, CT, 2009.
(71) Thom, H.; Dunning, J. *J. Chem. Phys.* **1989**, *90*, 1007−1023.
(72) *TURBOMOLE*, V6.5 2012, a development of University of Karlsruhe and Forschungszentrum Karlsruhe GmbH, 1989−2007; TURBOMOLE GmbH, http://www.turbomole.com (accessed April 2016).
(73) Weigend, F.; Häser, M. *Theor. Chem. Acc.* **1997**, *97*, 331−340.
(74) Finley, J.; Malmqvist, P.-Å.; Roos, B. O.; Serrano-Andrés, L. *Chem. Phys. Lett.* **1998**, *288*, 299−306.
(75) Forsberg, N.; Malmqvist, P.-Å. *Chem. Phys. Lett.* **1997**, *274*, 196−204.
(76) Langhoff, S. R.; Davidson, E. R. *Int. J. Quantum Chem.* **1974**, *8*, 61−72.
(77) Pople, J. A.; Seeger, R.; Krishnan, R. *Int. J. Quantum Chem.* **1977**, *12*, 149−163.
(78) Aquino, A. J. A.; Barbatti, M.; Lischka, H. *ChemPhysChem* **2006**, *7*, 2089−2096.
(79) Coccia, E.; Guidoni, L. *J. Comput. Chem.* **2012**, *33*, 2332−2339.
(80) Barborini, M.; Guidoni, L. *J. Chem. Theory Comput.* **2015**, *11*, 508−517.
(81) CASPT3/ANO-L-VTZP calculations of excitation energies using 0-IPEA were only successful for a two-root SA-CASSCF wave function. For a three-root SA-CASSCF wave function, the calculations failed with 0-IPEA. On the other hand, CASPT3/ANO-L-VDZP using a three-root SA-CASSCF wave function as a reference completed successfully in both cases with 0-IPEA and S-IPEA (see Tables S8 and S9 in the Supporting Information), but as pointed out in the present paper, the ANO-L-VDZP basis set is not sufficiently extensive to provide reliable results in CASPT3 calculations. Therefore, in the discussion of the effect of the IPEA parameter on the excitation energies, we only consider CASPT3/ANO-L-VTZP results.

DOI: 10.1021/acs.jctc.6b00108
J. Chem. Theory Comput. 2016, 12, 2346−2356